Histology Atlas and Systematic Approach to Postmortem Examination of the Queen Conch Lobatus gigas

Authors: Tiley, Katie, Freeman, Mark A., Yen, Irene, and Dennis, Michelle M.

Source: Journal of Shellfish Research, 38(1) : 131-148

Published By: National Shellfisheries Association

URL: https://doi.org/10.2983/035.038.0113

Journal of Shellfish Research, Vol. 38, No. 1, 131–148, 2019.

HISTOLOGY ATLAS AND SYSTEMATIC APPROACH TO POSTMORTEM EXAMINATION OF THE QUEEN CONCH *LOBATUS GIGAS*

KATIE TILEY, MARK A. FREEMAN, IRENE YEN AND MICHELLE M. DENNIS*
Center for Conservation Medicine and Ecosystem Health, Ross University School of Veterinary Medicine, West Farm, Basseterre, St. Kitts and Nevis

ABSTRACT The queen conch *Lobatus gigas* is the second largest commercial fishery in the Caribbean, and overharvesting has resulted in significant population declines. Depleted populations are at greater risk of stochastic events, including disease epidemics; however, disease diagnosis in *L. gigas* has been limited by the lack of standard procedure and histological reference material. This manual outlines a systematic technique for postmortem examination and compiles a comprehensive histology atlas to facilitate research regarding the pathology of *L. gigas*. Methods for euthanasia, dissection, sampling, and fixation are described, which produced optimal presentation and preservation of tissues. The recommended approach includes anesthesia with magnesium sulphate, extraction from shell, and euthanasia by incision through ganglia posterior to the buccal mass, followed by exposure of all tissues using four incisions. Anatomy is described for both sexes and standard sample locations are established. Tissue fixation is optimal using Davidson's formula. A histological reference for 16 tissues, nine of which were described for the first time in this species, is presented, including the anus, columellar muscle, digestive gland, esophagus, foot, ganglia and nerves, gill, gonad, heart, hypobranchial gland, kidney, mantle, nephridial gland, osphradium, small intestine and rectum. This manual is the first necropsy guide and histology atlas for *L. gigas*, a baseline resource for researchers monitoring health and disease in the species.

KEY WORDS: histology, queen conch, *Lobatus gigas*, *Strombus gigas*, postmortem examination, histopathology, gastropod, mollusc

INTRODUCTION

Queen conch *Lobatus gigas* (Linnaeus, 1758) formerly *Strombus gigas* is a large marine gastropod distributed throughout the tropical northwestern Atlantic. They are long-lived benthic herbivores and detritivores that typically inhabit sea grass beds and reach 20–40 y of age. Sexual maturity is reached at approximately 3–4 y of age, making the queen conch vulnerable to exploitation.

Fished for its meat and shell, the species makes up the second largest Caribbean fishery; its export trade is valued at 60 million US dollars (Theile 2003) and is only exceeded by the spiny lobster *Panulirus argus* (Brownell & Stevely 1981). Since a peak in 1995, catches have shown a progressive decline attributed mostly to overfishing. Some stocks have been severely depleted and not yet recovered following decades of fisheries restrictions (Appeldoorn 1994, FAO 2012, FAO 2017, Stoner et al. 2018). The sustainability of the fishery is increasingly questioned, and the species is listed in Appendix II of the Convention on International Trade in Endangered Species which highlights a worsening situation. Mariculture of the queen conch involves collection of egg masses from spawning aggregation sites and growing larvae and juveniles until harvest size is reached. Commercial farming is not yet economically viable because of the time required for growth and the limited understanding of *Lobatus gigas* nutritional requirements. Depleted populations are at a high risk for total elimination by disease outbreaks or environmental issues (De Castro & Bolker 2004), yet there is limited literature regarding diseases of the conch, which may put these depleted populations at further risk or present further impediments to successful mariculture.

*Corresponding author. E-mail: midennis@rossvet.edu.kn
DOI: 10.2983/035.038.0113

Investigations in *Lobatus gigas* are limited by the paucity of literature addressing not only pathology but also normal anatomy and histology of the species. Descriptions of the appearance of normal tissues and cells are necessary baselines to which samples from diseased animals are compared. Only the histology of select organs, including the foot, buccal mass, verge (penis), anus, gill, style sac, kidney, gonad, and digestive gland, has been described (Avila-Poveda et al. 2003, Delgado et al. 2004, Avila-Poveda et al. 2005, Gros et al. 2009). No published reports suggest methods for dissecting and gross examination of *L. gigas* tissues, and none detail normal microscopic anatomy, elements essential for conducting a comprehensive assessment. The literature describing known lesions of the queen conch can be summarized as follows. A condition known as imposex where the females grow a pseudopenis and become reproductively nonviable is believed to result from tributyltin exposure (O'Neal et al. 2011). Foci of inflammation in the muscle of *L. gigas* have been grossly evident as orange-colored protrusions and were thought to be caused by digenean parasites (Cuartas et al. 2018). Metazoan parasites also thought to be digenean cercaria were microscopically evident in the digestive gland, gill, rectum, and mantle of around 5% of *L. gigas* in St. Kitts (Tiley et al. 2018a). Inflammation of the mantle may present as a nodule filled with caseous exudate (Tiley et al. 2018a). Proliferation of nerve fibers and neuronal apoptosis and loss were described in a population affected with reproductive failure (Glazer et al. 2008). High zinc levels were associated with testis regression in this population and postulated to inhibit reproduction (Spade et al. 2010). Pathogenic bacteria, including *Klebsiella pneumonia* spp. *rhinoscleromatis* and *Photobacterium damselae*, have been isolated from *L. gigas* (Rodriguez et al. 2011), but their significance was unclear.

This manual outlines a standardized postmortem examination guide and establishes a comprehensive histology atlas for *Lobatus gigas* to facilitate disease diagnosis and aid the

efforts to develop sustainable fishing practices and stock recovery. It is built upon previous descriptions of *L. gigas* histology (Avila-Poveda et al. 2003, Delgado et al. 2004, Avila-Poveda et al. 2005, Gros et al. 2009), providing a comprehensive description of a complete assortment of tissues, while also accounting for sampling factors that may affect histology quality. The methods recommended by this manual were devised through trial and error while examining 76 conches, sourced through local fishermen, and collected within legal size and weight restrictions of St. Kitts and Nevis following the fisheries regulations (Heyliger 1995). Comparisons among dissections and existing literature guided the description of gross anatomy. Anesthetics were compared for their ability to induce nonresponsiveness in *L. gigas*, as indicated by a relaxed columellar muscle, allowing the buccal mass and foot to protrude from the aperture of the shell. A variety of fixatives were compared for their ability to preserve tissue architecture and cellular detail. Recommendations for tissue sampling for histology reflect those locations that provided adequate microscopic representation of essential anatomical features.

It is hoped that this manual will facilitate research and diagnoses in *Lobatus gigas*, essential for future conservation and aquaculture of this commercially valuable species. Research into the pathology of *L. gigas*, using the methods outlined here, is warranted in many areas of the Caribbean to improve the limited knowledge on issues that may threaten the species.

RECOMMENDED GUIDELINES FOR POSTMORTEM EXAMINATION

Euthanasia

A major challenge to the postmortem examination of *Lobatus gigas*, and gastropods in general, is extracting the host from its shell while minimizing host stress and tissue damage. Although this has obvious welfare implications, it can also drastically impact the assessment of tissues where stressed *L. gigas* produce copious quantities of mucus, complicating gross evaluation, histological processing, and preservation of tissue architecture. Therefore, a two-step anesthesia and pithing technique is recommended, following the recommendations of the American Veterinary Medical Association for aquatic invertebrates (Leary 2013), allowing the animal to be extracted from its shell with minimal stress before euthanasia.

Postmortem decomposition manifests artifactual tissue changes as soon as 20 min after the animal expired and substantially obscures pathology. Best results are achieved when harvested *Lobatus gigas* are held alive in saltwater until the necropsy can be performed, ideally the same day as harvesting to concomitantly minimize the potential for the host stress response.

Immerse conches in magnesium sulfate (3 g/4 L seawater) for 1–2 h to induce nonresponsiveness. Immersion in clove oil, ethanol, or greater concentrations of magnesium sulfate will also induce nonresponsiveness but will incite an intense mucus production and therefore are not recommended. The use of an ice bath, rather than chemical anesthesia, is not recommended because it will cause the hemolymph to pool in tissues, especially in the mantle and anus, and is less effective at inducing nonresponsiveness. Immersion in magnesium sulfate before extraction from the shell is time consuming, and a thorough study dedicated to methods of sedation and euthanasia could be beneficial for optimizing anesthesia protocols for queen conch, potentially exploring the options of intracoelomic administration of magnesium sulfate (Lewbart & Mosley 2012) or carbon dioxide bubbling (Cooper 2011).

In many marine invertebrates, examination of the hemolymph can supplement the postmortem examination, facilitating the rapid diagnosis of inflammatory conditions while histology is pending. Very little is known regarding the immune system and hemolymph of the queen conch. If hemolymph assessment is of interest, it would ideally be collected at this stage, while the conch is anesthetized.

Once the conch is removed from the shell, a 1-cm sagittal incision is made through the ganglia located immediately posterior to the buccal mass to complete euthanasia. As in other species, some muscular tissues may continue to contract postmortem. Although the cardiovascular and nervous systems cease to function at the time of death, muscle tissue may remain active until ATP is depleted and can be reflexively stimulated to contract.

External Examination

Morphometric measurements are recorded first and can be performed during the anesthesia step (Fig. 1). The shell of *Lobatus gigas* is spiralled with a right-handed opening, termed aperture, which is bordered by inner and outer lips. Growth of the shell occurs at the outer lip margin. The whorls of the shell together form the spire, except for the last and largest whorl, the body whorl. Each whorl is apparent by a row of spines on the surface of the shell. Calipers are used at the thickest point of the outer lip, typically in a central position, to measure lip thickness (Fig. 1B). Conches with lip thickness less than 15 mm are considered sexually immature (Stoner et al. 2012, Boman et al. 2018). The shell length is measured from the apex of the shell spire to the anterior (abapical) extremity, typically the siphonal canal (Fig. 1C). The siphonal canal is a notch-like extension of the aperture through which the left eyestalk often protrudes in a nonsedated animal. Queen conches are dioecious and show sexual dimorphism in the shell size. Shell length greater than 25 cm in females and greater than 23 cm in males may indicate sexual maturity (Avila-Poveda & Baqueiro-Cárdenas 2006). Lip thickness is considered a better indicator of sexual maturity than shell length (Avila-Poveda & Baqueiro-Cárdenas 2006, Boman et al. 2018). Whether the shell outer lip flares outward is also recorded as this is often used, perhaps inaccurately, as an indicator of sexual maturity (Stoner et al. 2012). Weight is recorded of (1) the combined body and shell, (2) the shell only postextraction, and (3) the internal viscera postextraction. In addition, the general type and coverage of epibiota on the surface of the shell are noted, which are broadly categorized into algae, seaweed, sponges, corals, barnacles, or bivalves. The inner shell is carefully examined for curvilinear or porous areas of decoloration or cracking of the nacre that may indicate the presence of boring organisms, such as clionid sponges.

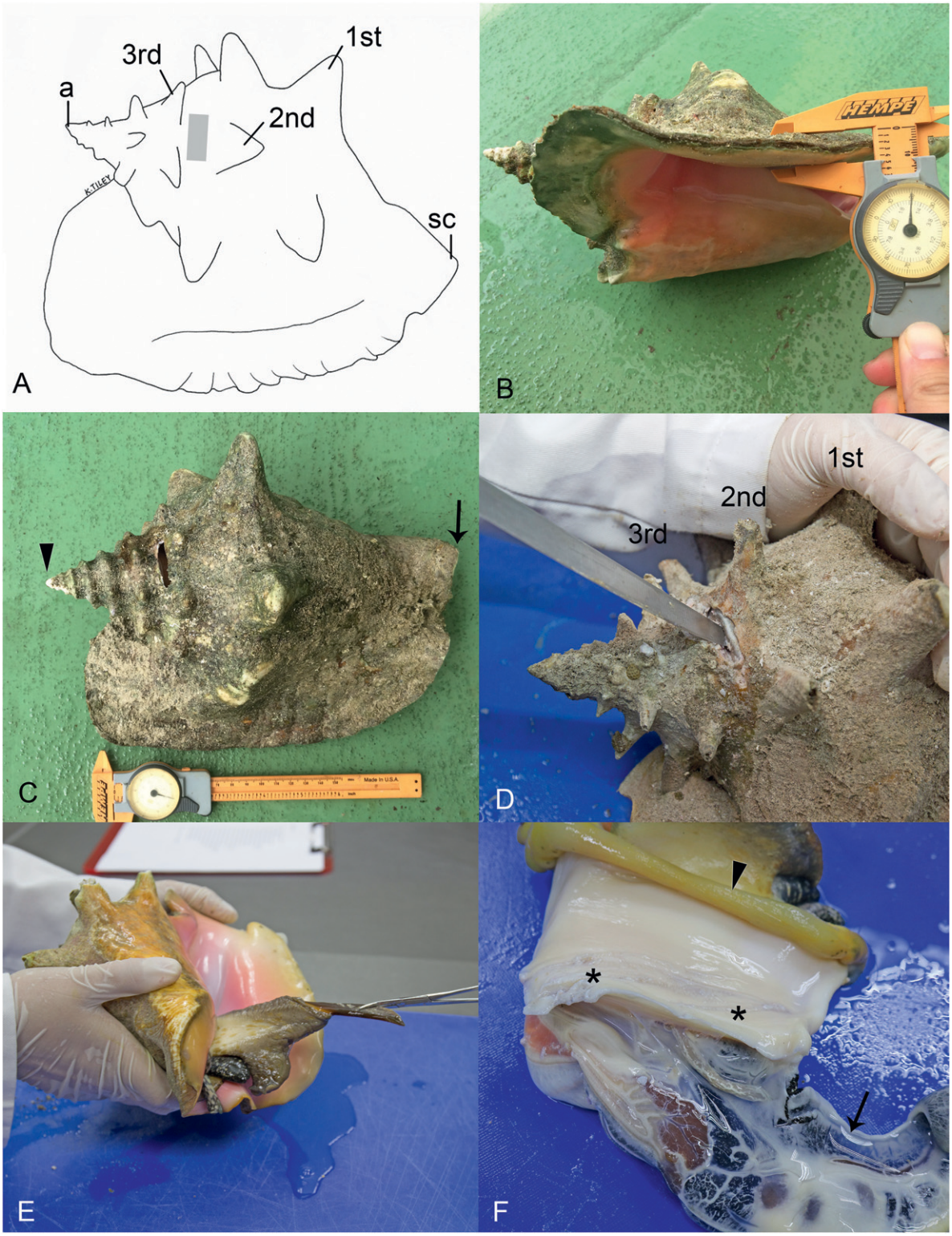

Figure 1. (A) External anatomy of a conch demonstrating the ideal position of a hole for severing the columellar muscle attachment, indicated by the gray area between the second and third row of spines. sc, siphonal canal; a, apex of the spire. Original artwork produced by Katie Tiley. (B) Lip thickness is the thickest point of the outer lip of the aperture of the shell, typically measured in a central position using calipers. (C) Shell length is the greatest straight length of the shell, taken from the apex of the spire (arrowhead) to the abapical extremity, in the region of the siphonal canal (arrow). (D) A straight blade is inserted into the shell hole at a 45° angle between the second and third row of spines and beneath the delicate viscera. (E) The operculum is grasped with hemostats, and steady traction at a perpendicular angle to the shell is applied to extract the conch. (F) The severed columellar muscle attachment (asterisks) on the underside of the conch when cut effectively. The arrowhead indicates the margin of mantle. The arrow indicates the visceral mass.

Shell Extraction

Extraction from the shell is stressful on the animal, and if sedation was unsuccessful, *Lobatus gigas* may contract and retreat further inside the shell. Therefore, initially, it is advisable to attach hemostats to the operculum or have a partner grip the operculum with one hand and brace against the anterior end of the shell with the other hand (Fig. 1D). The operculum is a horny and calcareous claw-like appendage at the posterior aspect of the foot, used for locomotion and as a durable closure for the mantle cavity when the body retracts (Voltzow 1994). This ensures that the animal is not "lost" inside the shell, meaning it can no longer be reached for extraction. In addition, the use of protective eyewear is advised as pieces of shell frequently dislodge and become airborne during the extraction process. To extract the gastropod from its shell, the columellar muscle must be severed from its attachment to the columella, the central axis of the shell. To do so, a thin rectangular hole is made on the dorsal aspect of the shell spire, approx. 3–5 cm in length and 1–2 cm in height between the second and third spine rows (Fig. 1A, D); in practice, either the claw of a hammer or a hammer and chisel achieve this effectively. Portions of the internal viscera, including the stomach, digestive gland, and gonads, may be partially viewed through this hole. Once the hole is made, a sharp straight blade is inserted beneath these viscera at a 45° angle against the inner ring of shell, the tip sliding along the columella. Once inserted as far as possible, slide the blade from side to side, staying close to the columella and severing the columellar muscle at its attachment. Leaking hemolymph (clear blue-tinged fluid) through the hole is a likely indication that the viscera have been lacerated, and one should proceed more carefully as the soft tissues coiled within the spire of the shell are very delicate and, if accidentally severed, can remain in the spire when the conch is removed from the shell. When the columellar muscle attachment is successfully severed, the operculum is grasped either directly or using the hemostats applied previously, and slow, steady traction is applied (Fig. 1E). Steady traction at a perpendicular angle to the shell reduces the chance of tearing the viscera and leaving the digestive gland and gonads within the shell. The animal should emerge slowly but smoothly for all tissues to remain intact; any sudden force could cause the coiled visceral mass contained in the spire to tear. An ideal cut during extraction will leave the severed columellar muscle attachment on the underside of the animal neat and straight (Fig. 1F).

Once extraction is successful, immediately complete the euthanasia procedure outlined previously by making a 1-cm sagittal incision through the ganglia located immediately posterior to the buccal mass.

Dissection

Before dissection and after extraction from the shell, the conch is orientated with the operculum toward the bottom left (in an 8 o'clock position), with the severed muscle attachment on the underside and the visceral mass on the bottom right (in a 4 o'clock position) when viewed from above (Fig. 2A, B). The visceral mass is a soft, coiled portion of dorsoposterior viscera normally contained within the spire of the shell, including the digestive gland, gonad, stomach, and kidney. The gonad of both sexes is situated at the apical margin of the black, digestive gland (Fig. 2B). They are usually a creamy-white color at rest

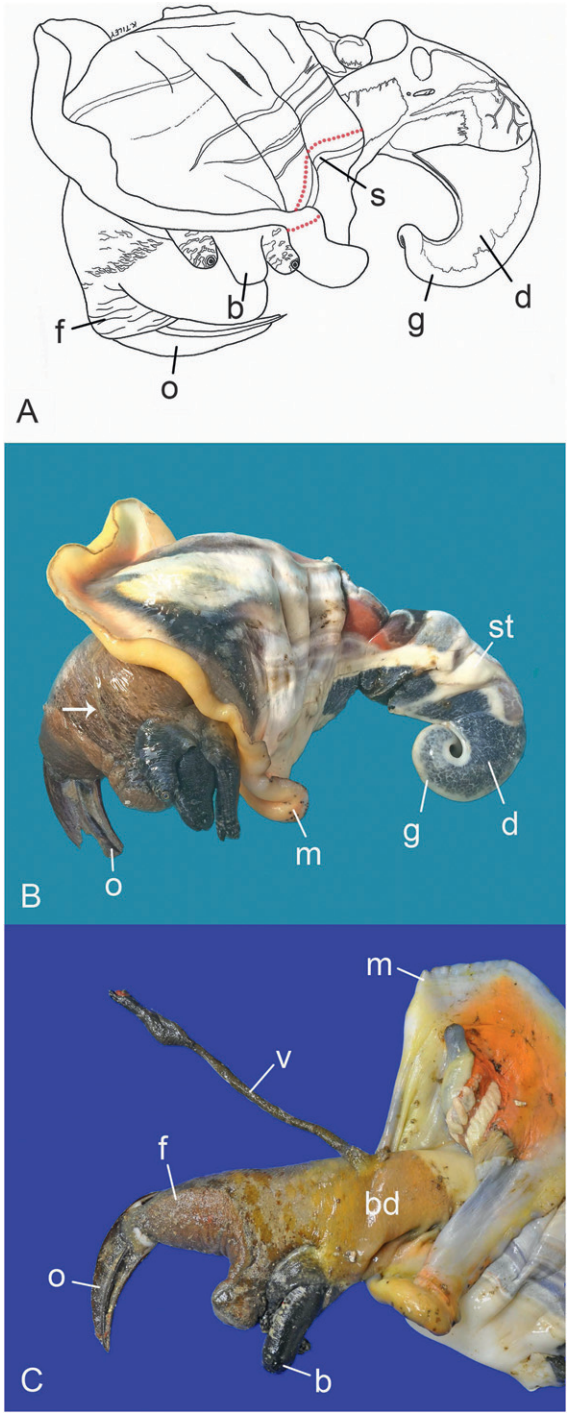

Figure 2. (A) The appearance of the conch once removed from the shell, positioned with the operculum (o) to the left and the visceral mass, including the digestive gland (d) and gonad (g), to the right. The red dotted line indicates the first incision from the edge of the mantle toward the viscera, following the dark gray style sac (s) until a blind corner is reached. b, buccal mass; f, foot. Original artwork produced by Katie Tiley. (B) Conch once removed from the shell, positioned with the operculum (o) to the left and the visceral mass, including the digestive gland (d) and gonad (g), to the right. In a female conch, an egg grove (arrow) courses along the surface of the columellar muscle toward the anterior foot. m, mantle; st, stomach. (C) Male conches are indicated by the presence of a verge (v). b, buccal mass; bd, body; f, foot; m, mantle; o, operculum.

but may appear yellow, orange, or even brick red (in males) when sexually active during the reproductive season (Tiley et al. 2018a). The sex of the conch can be determined at this stage by examining the body for the presence of an egg groove, which extends from the mantle wall through the surface of the columellar muscle to the foot margin, in females or a verge (or penis) in males (Fig. 2B, C). The dissector should consider whether there is imposex, evident by the presence of a pseudopenis in a female conch (confirmation in advanced cases may require histological sexing of gonad tissue) (Reed 1993). The mantle cavity is enclosed by the mantle, a thin skirt of rubbery tissue that is mostly cream-colored with patches of various shades of pale yellow, dark red, and gray (Fig. 2B). The mantle wall curves outward, distally following the curvature of the shell aperture, and its edges may have black-pigmented foci. The mantle should be carefully palpated for nodules that may represent foci of inflammation or mineral deposition (''pearls''). The crystalline style, a firm gelatinous rod of tissue that courses within the style sac, can also be palpated through the mantle (Fig. 3A). The body of the conch, consisting mostly of the columellar muscle, is partially exposed and partially concealed by mantle (Fig. 2C). Where exposed, the body surface is typically tan-brown, and there is often a distinct transition to paler coloration within the mantle cavity. Distally, the columellar muscle extends into the foot (Fig. 2C). The buccal mass, consisting of two eyestalks and the mouth, is on the body just proximal to the foot (Fig. 2).

The first incision of the dissection is made from the edge of the mantle toward the viscera, following the left-hand side of the style sac (Figs. 2A and 3A). The style sac can be identified as a dark gray linear area, slightly raised relative to the surrounding mantle tissue, which courses toward the stomach, perpendicular to the mantle edge. Often, the wall of the style sac is severed during extraction from the shell, revealing the crystalline style and facilitating identification of the style sac (Fig. 3A). Continue the cut until a blind corner, or a small triangular opening, is reached (Fig. 3B). Reflect the mantle cavity wall to the left-hand side, exposing the gill, osphradium, hypobranchial gland, rectum, and anus within the inner surface of the mantle cavity wall, each coursing parallel to the style sac. Characteristic of the clade Caenogastropoda (previously the Order Monotocardia), *Lobatus gigas* have a single gill or ctenidium. The osphradium, a chemosensory organ used by gastropods to locate food, mates, and predators, is regressed in *L. gigas* (Voltzow 1994) but is evident as a thin orange line parallel to the gill on the opposite side to the hypobranchial gland. The hypobranchial gland is a wrinkled cream-colored stripe of tissue located between the gill and rectum. If there was perimortem stress or a long postmortem interval, copious mucus may be within the mantle cavity, a product of the hypobranchial gland.

For the second incision, a V-shape cut is placed through the pericardial sac, along each edge of the heart (Fig. 3C). This incision creates a triangular flap of tissue that when retracted exposes the heart in a pool of blue-tinged hemolymph. This pericardial space is also referred to as a hemocoel (Voltzow 1994), and the heart consists of one auricle and one ventricle in *Lobatus gigas*. This stage of dissection presents another opportunity to collect hemolymph if its analysis is required.

The third incision is made by continuing down the right-hand side of the triangular flap of the pericardial sac. This incision courses along the right edge of the adjacent dark red brown area of tissue, which represents the outer surface of the nephridial gland and kidney (Fig. 3D), and proceeds to the edge of the viscera. Returning to the pericardial flap, that incision is extended in the other direction around the dark red brown area, again proceeding to the edge of the viscera, to produce a U-shaped incision and a semilunar flap of tissue. The flap of tissue is opened and laid flat to expose the kidney, nephridial gland, and the coiled loop of the small intestine (Fig. 3E). The apex where the small intestine turns 180° on itself is grasped with the forceps, unfolded, and extended to lay flat. Typically, the kidney is brown, and the nephridial gland is slightly more orange-tan. The shade of brown coloration to the kidney varies, but this was not associated with any microscopic differences in the tissue (Tiley et al. 2018a).

At this stage, the external surfaces of all viscera can be visualized (Fig. 4). The fourth and final incision is placed into the body of the conch, in the esophageal groove, a cavern in the columellar muscle that contains the esophagus. This incision extends from the incision placed posterior to buccal mass for euthanasia purposes toward the stomach (encompassed by the digestive gland) and follows a slightly depressed strip of body indicative of the esophageal groove (Fig. 3F). Once opened, the thin-walled brown esophagus and adjacent pale yellow-colored ganglia are visualized within the esophageal groove (Fig. 3F). A detailed figure of individual ganglia and commissures can be found in the article by Little (1965).

Careful examination is now being directed toward the reproductive tract. In males, a small orange sperm groove proceeds from the base of the verge along the body surface until it reaches the mantle, where it becomes the thicker cream-colored prostate (Fig. 4A) (Reed 1995a). The prostate runs parallel to the rectum and gills toward the internal viscera, where it develops into the vas deferens and becomes incorporated with the tubules in the coiled gonad tissue (Fig. 4A). In females, the thin, orange egg groove travels from its tip near the foot along the surface of the columellar muscle to the mantle, where it becomes the thicker, cream-colored uterine terminus (Fig. 4B) (Reed 1995b). This main tract divides into the thinner seminal receptacle, where spermatozoa received at copulation may be stored, and the more substantial winding uterine tract (also referred to as the pallial oviduct). Both structures run parallel to the rectum and gill toward the internal viscera. Within the mantle cavity and proximal to the internal viscera, the main uterine tract then branches sequentially into the spherical uterine ball and the spongy bursa copulatrix. The latter is a blind pouch where the male attaches the verge and from where spermatozoa received at copulation are passed on to the seminal receptacle. Last, there is the uterine apex, a looped projection of the reproductive tract that extends into the internal viscera and is incorporated beneath the kidney and nephridial gland. Oviducts extend from the uterine apex to the gonad in the coiled visceral mass. In reproductively active females, all uterine elements may be enlarged, reflecting the activity of a variety of glands, variably referred to as ''albumin,'' ''jelly,'' or ''capsule'' glands (Hyman 1967), together providing the secretions in which eggs are suspended or encapsulated in during ovipositioning.

A concluding step in the dissection is to open all alimentary lumina so that mucosal surfaces may be examined. The mouth is opened, exposing the radula. The style sac, a feature of herbivorous gastropods that courses in the mantle wall parallel to the esophagus, is opened. The crystalline style should be

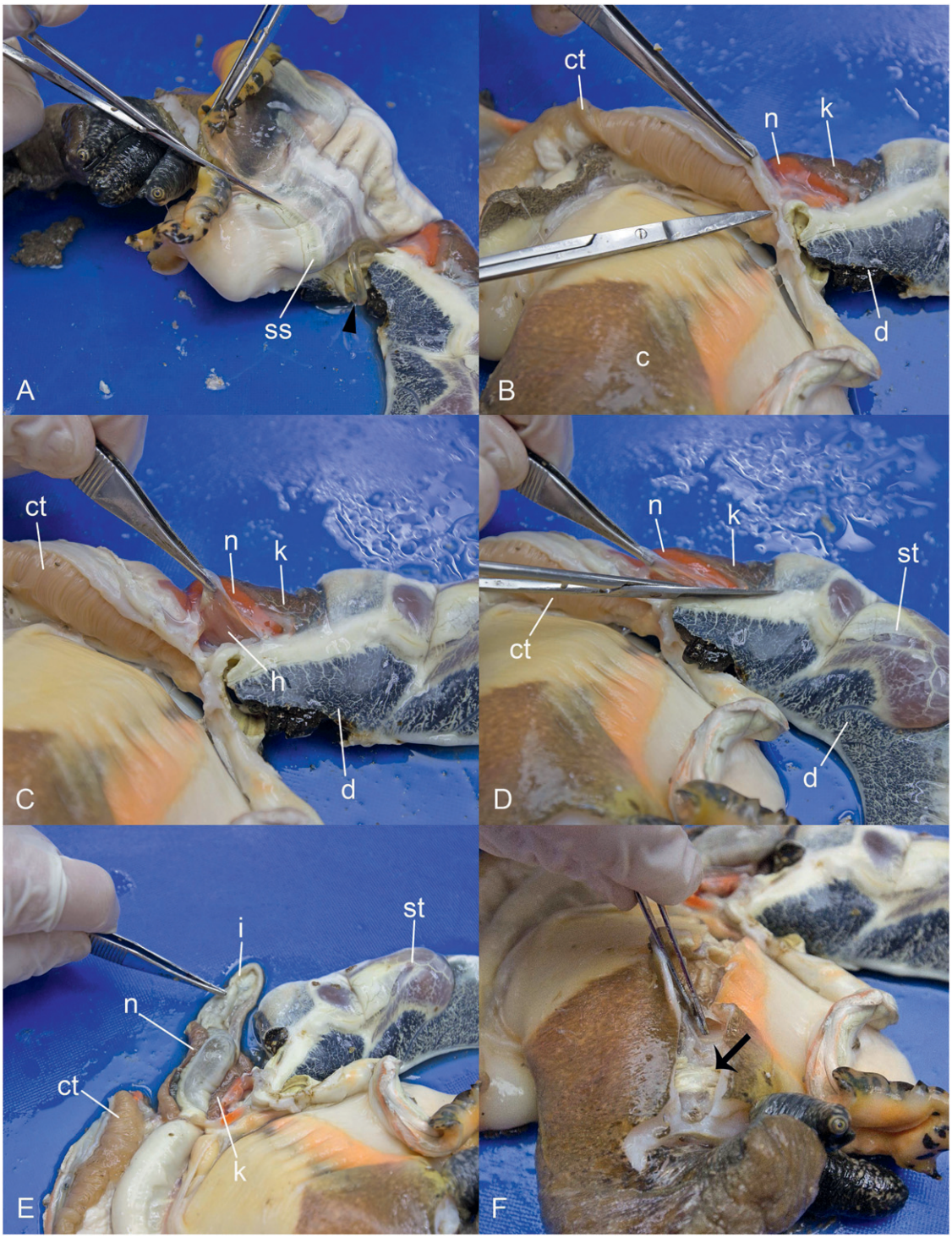

Figure 3. (A) The first incision extends from the mantle edge toward the inner viscera, following the left side of the style sac (ss). If the style sac has been severed during extraction from shell, the crystalline style will be visualized (arrowhead). (B) The first incision extends until the mantle cavity terminates in a blind corner adjacent to the ctenidium (gill, ct), nephridial gland (n), kidney (k), and digestive gland (d). c, columellar muscle. (C) The pericardial sac is opened by inserting scissors into the termination of the mantle cavity during the second incision, proximal to the kidney (k) and nephridial gland (n) and making a V-shaped incision to produce a triangular flap of tissue, which when lifted, exposes the heart (h). ct, ctenidium; d, digestive gland. (D) The third incision, an elongation of the second, is extended through the edge of the pericardial sac and continues along the border of the red brown area representing the external surfaces of kidney (k) and nephridial gland (n), producing a U-shaped incision. ct, ctenidium; d, digestive gland; st, stomach. (E) A semilunar flap produced from the U-shaped incision is reflected to expose the nephridial gland (n) and kidney (k), and the loop of small intestine (i) is unfolded and extended. ct, ctenidium; st, stomach. (F) The final incision opens the esophageal groove. Scissors are inserted into the euthanasia incision and extended toward the stomach through the slightly depressed area of the body where there is a cavity in the columellar muscle. Once opened, neural tissue is identified by its yellow color (arrow).

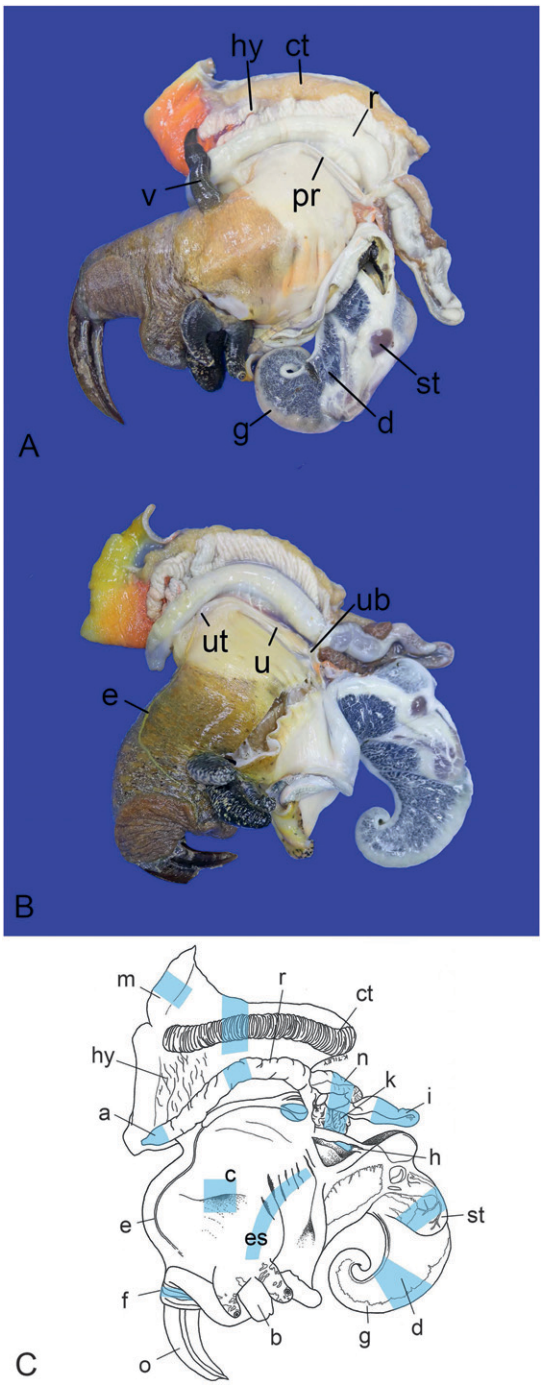

Figure 4. Exposed male reproductive tract postdissection, with the alimentary tract lumina unopen. The prostate (pr) runs parallel to the rectum (r). ct, ctenidium; d, digestive gland; g, gonad; hy, hypobranchial gland; st, stomach; v, verge. (B) Exposed female reproductive tract postdissection, with alimentary tract lumina unopen. The egg groove (e) extends from the foot to the mantle, where it transitions to form the uterine terminus (ut), which continues as the uterine tract (u), and forms the uterine ball (ub) within the mantle cavity. (C) The appearance of a female queen conch postdissection. The blue-shaded areas indicate locations from which samples for histology are typically collected. a, anus; b, buccal mass; c, columellar muscle; ct, ctenidium; d, digestive gland; e, egg groove; es, esophagus; f, foot; g, gonad; h, heart; hy, hypobranchial gland; i, small intestine loop; k, kidney; m, mantle; n, nephridial gland; o, operculum; r, rectum; st, stomach. Original artwork produced by Katie Tiley.

translucent and resilient, and it should extend into the stomach and appose itself against the cuticularized gastric shield. The stomach, small intestine, rectum, and anus (Fig. 4C) are longitudinally opened. The small intestine transitions into rectum, where it becomes incorporated into the mantle wall, running parallel to the hypobranchial gland and gill. The anus protrudes from the mantle wall approximately 1 cm from its margin.

Tissue Sampling and Fixation for Histology

A standardized sampling approach for histology is recommended (Fig. 4C), and the features described in this histology atlas were observed at these sampling locations. In a survey of *Lobatus gigas* pathology, pathology most frequently involved the digestive gland, gonad, kidney, mantle, gill, and rectum (Tiley et al. 2018a). Thus, histopathology efforts should be focused toward these tissues and those with important health implications (such as nervous tissue and heart), where resources are limited. A comprehensive assessment includes these organs as well as foot and columellar muscle, nephridial gland, esophagus, stomach, small intestine, rectum, and anus. As a general rule, the tissue fixative will diffuse no more than 0.5 cm; thus, a tissue sample for histology should not exceed 1 cm in thickness at its thinnest dimension.

The digestive gland and gonad are together sampled at a position where the visceral coil is approximately 3 cm in width, a site known to provide accurate representation of reproductive activity (Stoner & Brown-Peterson 2012). Luminal organs (i.e., intestine) are taken as segments to include full thickness representation of the wall of the tissue. Where segments are longer than 1 cm, it is important to open the lumen, if not already performed, such that the inner mucosal surface can be properly preserved by a fixative. Esophagus and adjacent nervous tissue are together sampled from the length of the esophageal groove, producing a thin ribbon of tissue 4–5 cm long. The ganglia of gastropods are often pigmented, facilitating their identification in fresh dissections (Voltzow 1994). In *Lobatus gigas*, ganglia are often pigmented yellow. Take care to extract one of the paired buccal ganglia immediately posterior to the buccal mass and the visceral ganglion on the wall of the esophageal groove close to the pericardial sac. Ganglia can also be sampled by transecting a 1-cm^3 portion of the surrounding columellar muscle. The gill, osphradium, and hypobranchial gland can be taken together in a selection of mantle tissue 1 cm from the mantle edge, at the border of the first incision made during the dissection. It is advised to exclude the hypobranchial gland for routine histology, however, because it adds little value to a pathology assessment and it will produce copious amounts of mucus during fixation, complicating processing for histology. Another portion of mantle is collected from the mantle edge and will provide a histological view of the mantle edge glands which produce the shell. The kidney, small intestine, and nephridial gland can also be collected together in a single sample but may also include a portion of uterine apex in mature females.

While sampling for histology, an extra set of nonfixed tissue samples can also be collected to facilitate the diagnosis of bacterial, fungal, and parasitic etiologies. Microbiological cultures can be prepared and tissue wet mounts or imprints can be examined with microscopy for infectious organisms. Where

etiology is uncertain, samples can be refrigerated or frozen while histological assessment is pending. An extra set of tissues may also be preserved in 95% ethanol if techniques involving genetic material will be undertaken. As we are only starting to elucidate the microbiota of *Lobatus gigas* tissue and the methods best suited to identify them (Pérez-Carrascal et al. 2014), diagnosticians are advised to consider techniques that are most capable of identifying marine bacteria (Joint et al. 2010).

Davidson's solution (Howard & Smith 1983) is recommended for fixation of tissues that will be evaluated using histology. It produces far superior preservation of cellular detail and staining quality relative to 10% neutral-buffered formalin with and without saline, zinc-buffered formalin in saline, 70% ethanol in saline, and a 1:9 ratio of 35% formaldehyde and 80% ethanol in saline. A major problem of solutions containing formaldehyde is the copious postsampling production of mucus by the tissue samples, not limited to mucosal surfaces. Solutions containing ethanol produce less mucus than those without and could be considered in situations where Davidson's solution is not available.

HISTOLOGY ATLAS

Mantle

A transverse section is prepared through the mantle to include the mantle edge (Fig. 5A). The mantle is covered by epidermis on both sides as it is essentially a fold of the body wall. Simple tall cuboidal to columnar epithelial "epidermal" cells, which may be pigmented, interspersed with mucus cells and ciliated cells, make up the epidermis (Fig. 5B, C) (Voltzow 1994). The epidermis of the inner or ventral mantle surface is continuous with the epidermis of the body of the conch, contains numerous mucus cells, and may form folds in *Lobatus gigas*, whereas the epidermis of the outer mantle surface, continuous with the exterior surface of the visceral mass, has sparse mucus cells, shorter epidermal cells, and may be more heavily sinuated while typically not forming folds (Hyman 1967). The subcutaneous tissue consists largely of loose fibrous connective tissue containing interwoven smooth muscle cells, Leydig cells, and hemolymphatic vessels. Leydig cells are glycogen-storing and mucus-producing stromal cells common among connective tissues of gastropods. In addition, mantle edge glands, responsible for the production of the shell, may be observed (Fig. 5A). Composed of tubules of tall cuboidal epithelial cells arranged into acini, these glands secrete extrapallial fluid in which shell formation occurs by emptying to the surface directly without a duct (Wilbur 1972).

Body and Foot

A longitudinal section of the body of the conch, parallel to the elongate body shape and perpendicular to the line of demarcation in the surface pigmentation of the body, is prepared for examining the columellar muscle and the integument of the body. The body is covered by epidermis, similar to the epidermis covering the mantle (Fig. 5D). Otherwise, the body is composed of dense collagenous connective tissue and interwoven and branching bundles of smooth muscle cells (the columellar muscle) and interspersed Leydig cells (Fig. 5E).

The foot is observed in a transverse section (i.e., perpendicular to the elongate shape of the foot), through the posterior region where it is adjacent but not attached to the operculum, such that the section produced circumferentially bears an epidermal surface. The foot is an extension of the columellar muscle and, thus, has internal composition similar to the body of the conch (Fig. 5E); however, the epidermis varies because of its locomotor function (Avila-Poveda et al. 2003). The foot epidermis is similar to the inner mantle epidermis and may have pronounced grooves throughout (Fig. 5F), especially on the sole. The sole is also thicker, with pseudostratified columnar cells that are often ciliated (Avila-Poveda et al. 2003, Avila-Poveda et al. 2005). Various glands, together termed pedal or suprapedal glands, are commonly found at the anterior end of the gastropod foot, just beneath the buccal mass, and the mucus produced by these glands is thought to lubricate the sole and facilitate locomotion. In *Lobatus gigas*, a pedal gland consisting of accentuated folds of epidermis, where ciliated simple columnar epithelial cells form deep mucus-filled valleys, has been described (Avila-Poveda et al. 2003, Avila-Poveda et al. 2005) but would not be featured in the area of foot sampled as per Figure 4C.

Digestive System

Luminal organs are typically examined in transverse section to examine all layers of the wall of the organ. Because of its thin and delicate wall, the esophagus may curl up during fixation; therefore, the esophagus should be left in association with adjacent nerves and ganglia, and serial transverse sections are prepared through these tissues together, potentially including adjacent columellar muscle.

The esophageal mucosa is arranged into longitudinal folds and is composed of simple columnar ciliated epithelial cells interspersed with mucus cells, especially at the tips of the folds (Fig. 6). Vascular loose fibrous connective tissue comprises the submucosa. The muscularis is very thin. Smooth muscle cells are generally orientated in a circular pattern around the longitudinal axis of the organ. Finally, the adventitia consists of vascular loose fibrous connective tissue that contains many nerve plexuses and Leydig cells. At the anterior end of the esophagus, the adventitia may feature sparse acini, representing salivary gland, lined by columnar mucus cells.

A transverse section is prepared from the stomach and may include a portion of the digestive gland, continuous with its adventitial surface on the posterior side where it is coiled into the spire of the shell. The mucosa is lined by simple columnar epithelial cells with microvillous border and occasional mucus cells. The mucosa may form ridges or folds near the esosphageal entrance, and in this area, ciliated cells predominate. In the region of the gastric shield, the mucosal surface is covered with a cuticle, a thin chitinous band that constitutes the gastric shield (Fig. 6C). The submucosa consists of loose fibrous connective tissue containing many hemolymphatic vessels and Leydig cells. Occasional cells containing faint gray-brown granules are present in the submucosa, as are scattered hemocytes (Fig. 6C). The muscularis blends with the submucosa, similarly consisting of circular-oriented smooth muscle cells. The external aspect consists of

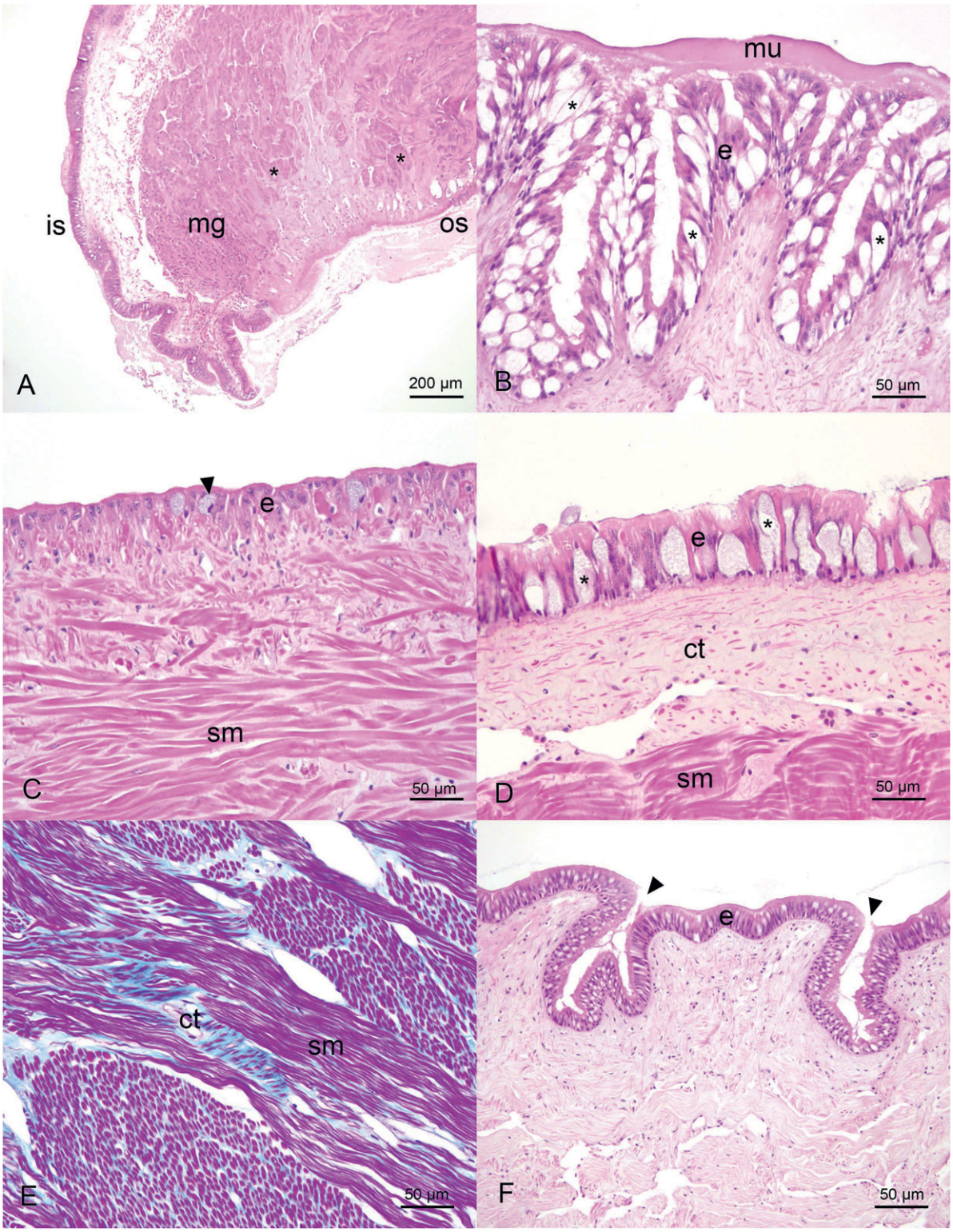

Figure 5. Mantle, body, and foot of *Lobatus gigas*. (A) The mantle edge is the convergence of the inner mantle surface (is) and outer mantle surface (os) where the mantle edge gland (mg) may be found. The gland is composed of tubules (asterisks) of cuboidal epithelial cells that empty onto the surface without a duct. Davidson's fixative, hematoxylin and eosin (HE) stain. (B) The inner mantle surface consists of epidermis (e), which contains many mucus cells (asterisks), and is often coated in mucoid secretion (mu). Davidson's fixative, HE stain. (C) The epidermis (e) of the outer mantle surface has fewer mucus cells (arrowhead) than the inner mantle surface. The subcutaneous tissue contains abundant smooth myocytes (sm). Davidson's fixative, HE stain. (D) The epidermis (e) of the body is similar to that of the inner mantle surface, including many mucus cells (asterisks). The body is composed mainly of smooth muscle cells (sm) and fibrous connective tissue (ct). Davidson's fixative, HE stain. (E) The bulk of the body consists of interwoven bundles of smooth muscle cells (sm) and fibrous connective tissue (ct). Davidson's fixative, Masson's trichrome stain. (F) The epidermis (e) of the foot sole forms grooves (arrowheads). Davidson's fixative, HE stain.

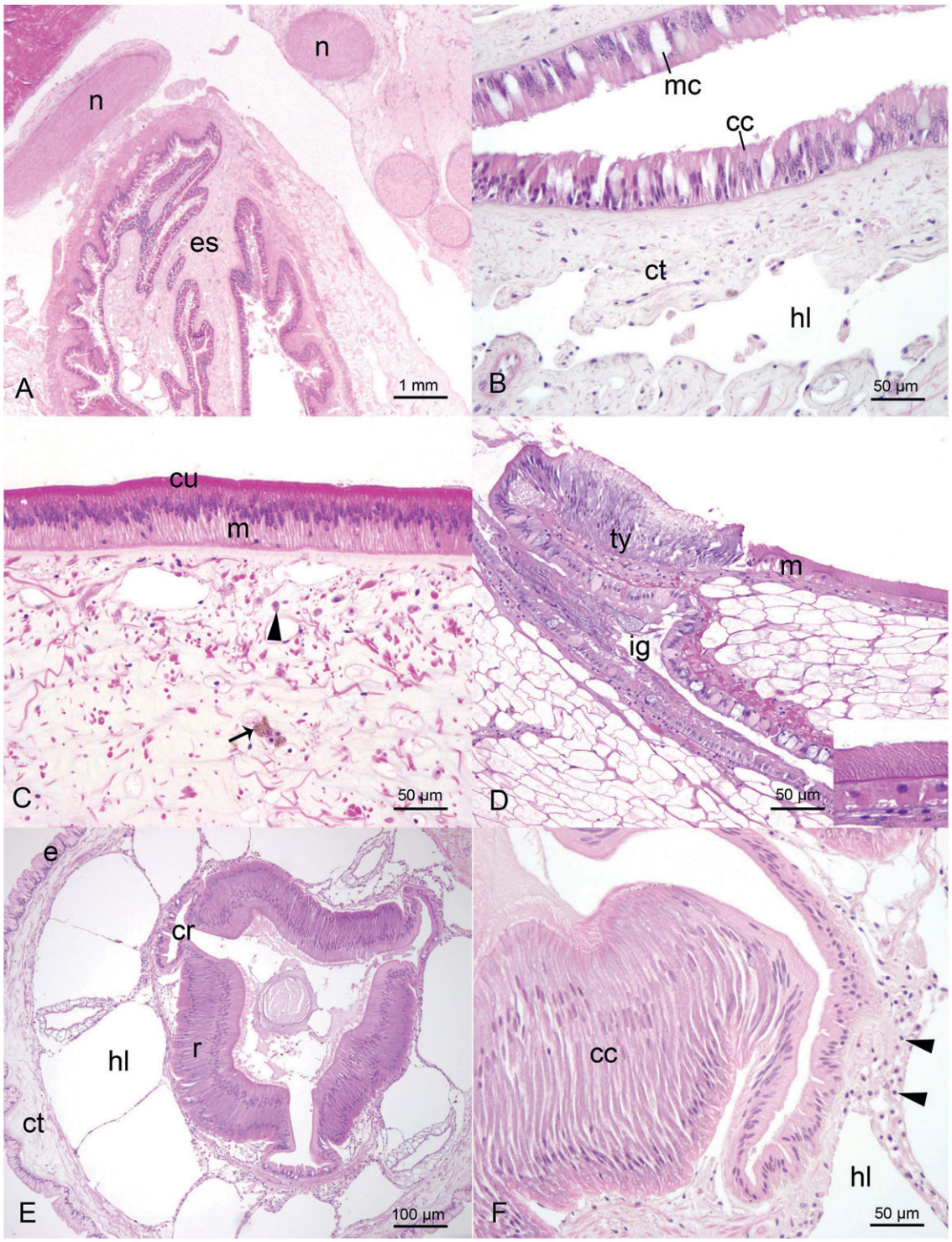

Figure 6. Esophagus, stomach, and small intestine of *Lobatus gigas*. (A) The esophagus (es) has a thin wall, and nerves (n) are closely associated with its adventitial surface. Davidson's fixative, HE stain. (B) The esophageal mucosa is lined by ciliated columnar epithelial cells (cc) and mucus cells (mc). The submucosa comprises loose fibrous connective tissue (ct) and contains many hemolymphatic vessels (hl). Davidson's fixative, HE stain. (C) In the region near the gastric shield, the gastric mucosa (m) is lined by simple columnar epithelial cells, which have a cuticle (cu). The submucosa is a loose fibrous connective tissue that contains hymolymphatic vessels and occasional hemocytes (arrowhead) and pigment-laden cells (arrow). 1:9 solution of 35% formaldehyde and 80% ethanol in saline, HE stain. (D) The style sac mucosa has a typhlosole (ty) containing a longitudinal intestinal groove (ig). The remaining mucosa (m) is lined by tall cuboidal acidophilic cells with long cilia (inset). 10% neutral buffered formalin in saline, HE stain. (E) The mucosa of the small intestine loop demonstrates longitudinal ridges (r) alternating with longitudinal crypts (cr). The submucosa is rich in hemolymphatic vessels (hl) and supported by loose fibrous connective tissue (ct). e, outer epidermal surface. Davidson's fixative, HE stain. (F) The mucosal ridges of the small intestine loop are composed of bilayered tall columnar ciliated epithelial cells with polar nuclei (cc). The submucosa consists of loose fibrous connective tissue containing many hemocytes (arrowheads) superficially and hemolymphatic vessels (hl). Davidson's fixative, HE stain.

integument, similar to the surface of the mantle and other viscera, containing simple columnar epithelial cells and mucus cells.

This species *Lobatus gigas* have a crystalline style, typical of microherbivorous gastropods (Salvini-Plawen 1988), contained within a style sac that opens near the esophagus on the anterior side of the stomach and can be examined microscopically in cross section, although not typically a focus for histopathology assessment or included in the samples of Figure 4C. The mucosa of the style sac has an obscure typhlosole (i.e., internal fold) with a central intestinal groove (Fig. 6D). Away from the typhlosole, the mucosa consists of tall cuboidal acidophilic columnar epithelial cells with long cilia (Fig. 6D inset). The typhlosole is lined by pseudostratified tall columnar ciliated epithelial cells. The intestinal groove is lined by simple columnar ciliated epithelial cells, admixed with mucus cells. The abundance of cilia within the stomach and style sac is important for generating ciliary currents, which sort and direct ingesta and rotate the crystalline style. The submucosa of the style sac consists of Leydig cells and sparse smooth muscle cells, with occasional pigmented cells and hemocytes, and it is exteriorly covered by epidermis, as for the stomach. The crystalline style consists of mucoglobulin (Hyman 1967) and microscopically appears as an amphophilic homogenous acellular substance cast within the lumen of the style sac.

The small intestine is arranged in a loop. A transverse section is prepared to span both sides of the loop, producing two profiles of small intestine. A transverse section of the anterior small intestine is also included in the section of kidney and nephridial gland. The mucosa of the small intestine is composed of bilayered tall columnar ciliated epithelial cells with polar nuclei, arranged into three longitudinal ridges. These ridges alternate with three longitudinal crypts lined by simple tall cuboidal to columnar epithelial cells (Fig. 6C and F). Loose fibrous connective tissue containing hemolymphatic vessels and Leydig cells comprises the submucosa, often containing faint gray-brown pigmented cells and many hemocytes superficially (Fig. 6F). The muscularis and external surface are as described for the stomach (Fig. 7A), but the epidermis is often thicker and more heavily sinuated.

The rectal mucosa (Fig. 7B, C) is composed of simple columnar epithelial cells, including granular mucus cells. In the authors' experience, epithelial cells frequently contain fine brown granular pigment, which stain blue with Perl's stain, indicating the presence of iron (Fig. 7C). The submucosa is similar to the small intestine, composed of loose fibrous connective tissue containing many hemolymphatic vessels and Leydig cells and superficial aggregations of hemocytes. The muscularis is poorly defined, composed of a thin layer of smooth muscle cells orientated in a circular pattern around the longitudinal axis of the organ (Voltzow 1994). The exterior epidermis of the rectum is integrated with the mantle epidermis and, thus, contains simple columnar epithelial cells interspersed with mucus cells (Fig. 7D). Because of the proximity to the hypobranchial gland, the epidermis is typically coated in a thick layer of mucoid secretion that can result in the artifactual disruption or loss of epithelial cells.

The anal mucosa consists of pseudostratified ciliated epithelial cells and many mucus cells (Fig. 7E, F). The submucosa is composed of loose fibrous connective tissue containing many hemolymphatic vessels, occasional nerve plexuses, and smooth muscle cells. As the anus emerges from the mantle, its exterior is composed of an epidermis similar to that of the mantle, a simple columnar epithelium with mucus cells interspersed, and may show longitudinal folds (Avila-Poveda et al. 2005, Avila-Poveda et al. 2006).

The digestive gland is typically examined in transverse section, including the gonad at one edge. Glands form branching tubules that supply secondary ducts (Fig. 8A, B). Much disagreement and confusion exist in the literature encompassing the digestive gland epithelial cells of prosobranchs (Hyman 1967). The cross section of a gland may show corners or indentations referred to as crypts (Gros et al. 2009). Two main cell types are recognized in prosobranchs: those within the crypts are referred to as secretory cells and those that are not are referred to as digestive cells (Voltzow 1994). Digestive cells are columnar or club shaped, have a microvillus border, and have apical vesicles. In *Lobatus gigas*, there are two types of secretory cells: pyramidal (or crypt) cells that are short, cone-shaped, and present in small groups, and vacuolated cells are taller and have vacuolated cytoplasm (Gros et al. 2009). Vacuolated cells and, perhaps, digestive cells to a lesser extent, frequently contain 15 × 30-µm, elongate to ovoid to tribulbous, and dark brown inclusion bodies. Initially interpreted as protozoan parasites (Baqueiro-Cárdenas et al. 2007, Gros et al. 2009), they were later demonstrated to contain iron, mineral, and melanin, but a variety of techniques failed to demonstrate parasite morphology or DNA (Tiley et al. 2018b). Similar inclusion bodies are present within the digestive gland epithelial cells of other members of the Strombidae family (Volland et al. 2010). It is presently hypothesized that these inclusion bodies have a role in element cycling, in line with similar granules or ''calcareous bodies'' observed in the digestive gland epithelial cells of other prosobranchs (Hyman 1967, Voltzow 1994). Smaller 10–12-µm spherical blue-gray to brown granules are often within the basal cytoplasm of digestive cells (Gros et al. 2009). Pyramidal cells also frequently have cytoplasmic 2–4-µm blue-brown granules, referred to as spherocrystals, a structure involved in mineral and trace metal homeostasis in Strombidae (Volland et al. 2012). It is unclear how or if all of these different types of granules or inclusions are related to one another. Secondary ducts are lined by simple columnar epithelial cells that have a microvillus border and show apocrine secretion. In some instances, these cells may have apical granules that stain for iron (Fig. 8B). The ducts culminate into two primary ducts that are larger and have plicated segments of pseudostratified ciliated columnar epithelial cells, with few interspersed mucus cells. Primary ducts empty into the stomach (Gros et al. 2009). The interstitium is composed of vascular loose fibrous connective tissue and Leydig cells.

Urinary System

A transverse section prepared across both the kidney and nephridial gland, including the anterior end of the small intestine loop connecting the tissues, is examined. In Caenogastropoda, the hemolymph passes through the wall of the heart, into the pericardial space, and to the nephridial gland through the nephridial duct (Voltzow 1994). It then returns to

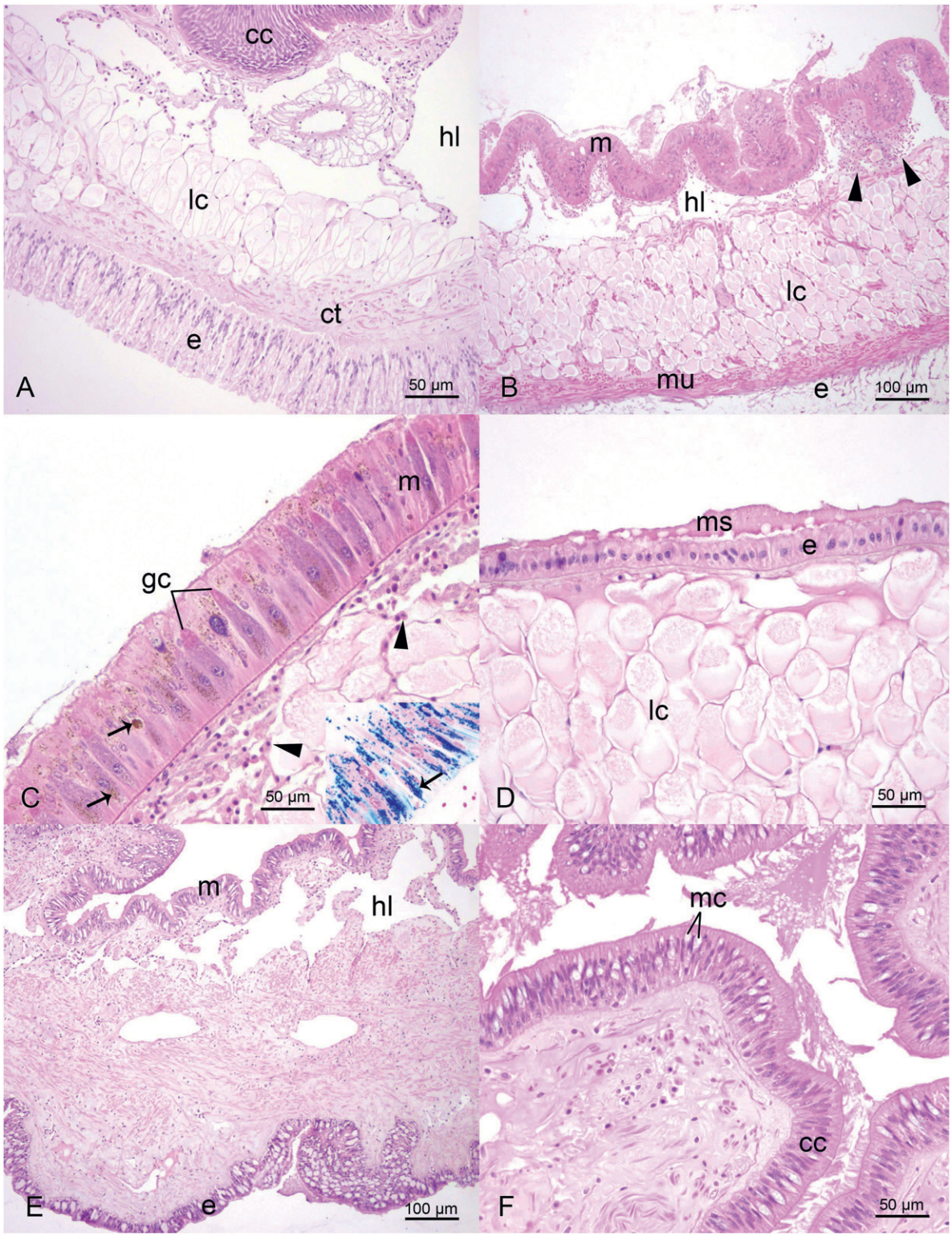

Figure 7. Small intestine, rectum, and anus of *Lobatus gigas*. (A) The external surface of the small intestine loop consists of epidermis (e). The mucosa is lined by columnar ciliated epithelial cells (cc). The submucosa consists of loose fibrous connective tissue (ct) containing many hemolymphatic vessels (hl) and Leydig cells (lc). Davidson's fixative, HE stain. (B) Transmural section of rectum showing mucosa (m), submucosa containing many hemocytes (arrowheads), hemolymphatic vessels (hl), and Leydig cells (lc), transitioning to a poorly defined muscularis (mu), and outer epidermal surface (e). Davidson's fixative, HE stain. (C) The rectal mucosa (m) shows granular mucus cells (gc) and iron granules within mucosal epithelial cells (arrows). The arrowheads designate hemocytes within the superficial submucosa. Davidson's fixative, HE stain; inset Perl's stain. (D) Exterior rectal epidermis (e) showing surface-associated mucoid secretion (ms) and submucosal Leydig cells (lc). Davidson's fixative, HE stain. (E) Transmural section of the anus showing mucosa (m), submucosa containing hemolymphatic vessels (hl), and outer epidermal surface (e). Davidson's fixative, HE stain. (F) The anal mucosa consists of pseudostratified ciliated epithelial cells (cc) and mucus cells (mc). Davidson's fixative, HE stain.

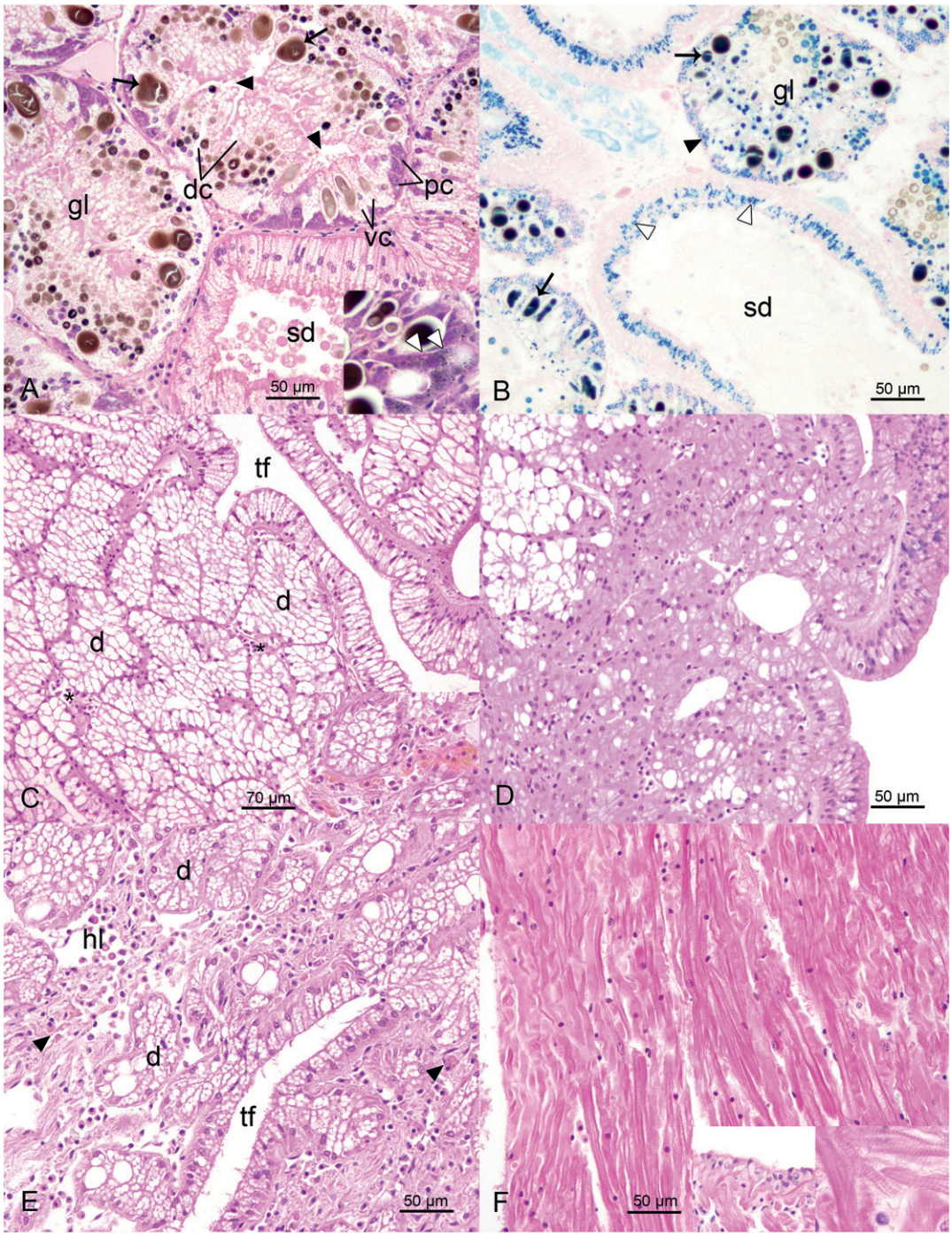

Figure 8. Digestive gland, kidney, nephridial gland, and heart of *Lobatus gigas*. (A) Tubules (gl) supply secondary ducts (sd) of the digestive gland. Tubules are lined by digestive cells (dc), and in crypt regions (black arrowheads), pyramidal cells (pc) and vacuolated cells (vc). Spherical to bulbous brown inclusions are often within digestive and vacuolated cells (arrows). The inset shows higher magnification of pyramidal cells demonstrating cytoplasmic spherocrystals (white arrowheads). Davidson's fixative, HE stain. (B) Digestive gland tubules (gl) supply secondary ducts (sd). Spherocrystals within pyramidal cells (black arrowheads), granules within secondary ductular epithelial cells (white arrowheads), some of the large granules within digestive cells, and the brown inclusion bodies (arrows) stain for iron. Davidson's fixative, Perl's stain. (C) The kidney is composed of columnar epithelial cells (nephrocytes) that form ducts (d) and line the organ surface, extending inward to tubular folds (tf), supported by sparse collagenous interstitium containing few hemolymphatic vessels (asterisks). Aggregates of pigmented cells are occasionally identified in the interstitium between ducts (inset). Davidson's fixative, HE stain. (D) Renal epithelial cells (nephrocytes) in the right of the figure comparatively lack cytoplasmic vacuolation. Davidson's fixative, HE stain. (E) Nephridial gland epithelial cells are very similar to the kidney, forming ducts (d) and tubular folds (tf), and the interstitium contains many hemolymphatic vessels (hl) and occasional pigmented cells (arrowheads). Davidson's fixative, HE stain. (F) Myocytes of the ventricular myocardium course mostly in parallel, leaving poorly defined fine trabecular hemolymphatic spaces. Inset (left) showing simple squamous epithelium lining the epicardial surface and (right) higher magnification of cardiac myocytes and their cross striation and apparent branching. Davidson's fixative, HE stain.

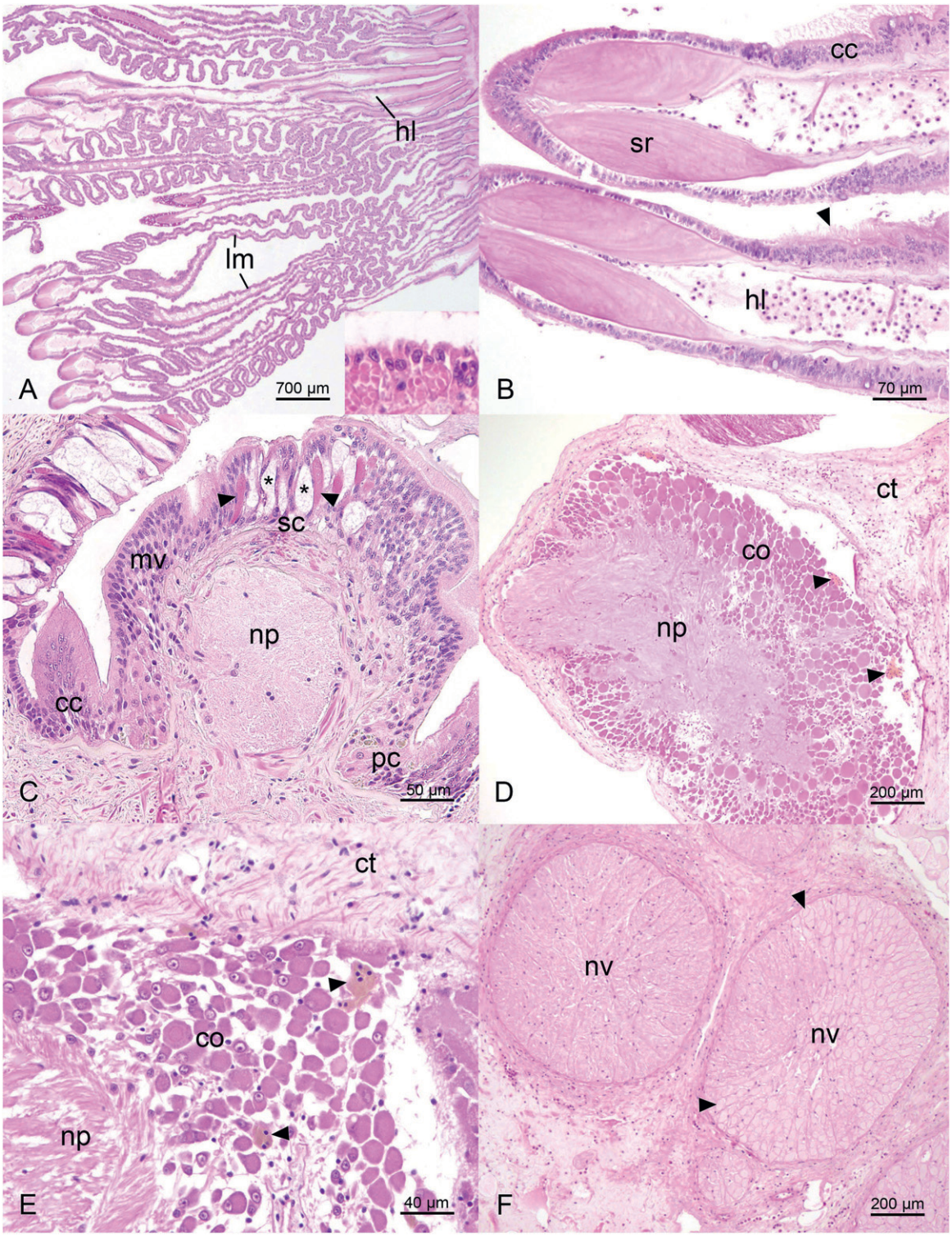

Figure 9. Gill, osphradium, ganglia, and nerves of *Lobatus gigas*. (A) The gill lamellae (lm) have central hemolymphatic vessels (hl). Lamellae are lined by a single layer of columnar to cuboidal cells interspersed with mucus cells and granular gland cells (inset). Davidson's fixative, HE stain. (B) The tips of gill lamellae are flared, have a zone of columnar epithelial cells (cc) with exceptionally long cilia (arrowhead), and are supported by skeletal rods (sr). hl; hemolymphatic vessels. Davidson's fixative, HE stain. (C) The osphradium sensory cup (sc) is composed of psueudostratified columnar cells interspersed with mucus cells (asterisks) and cells with homogenous eosinophilic cytoplasm (arrowheads). This area is bordered by columnar cells with a microvillus border (mv) and a peripheral ridge of pigmented cells (pc) and ciliated columnar cells (cc). np; neuropil. Davidson's fixative, HE stain. (D) Ganglia have a cortex (co) composed of neuronal cell bodies and a central zone of neuropil (np). There are aggregates of pigmented cells (arrowheads) and bordering fibrous connective tissue (ct). Davidson's fixative, HE stain. (E) Ganglia have a cortex (co) composed of neuronal cell bodies, a central zone of neuropil (np), aggregates of pigmented cells (arrowheads), and are bordered by fibrous connective tissue (ct). Davidson's fixative, HE stain. (F) Nerves (nv) examined in cross section may show circular profiles resembling large axons (arrowheads). Davidson's fixative, HE stain.

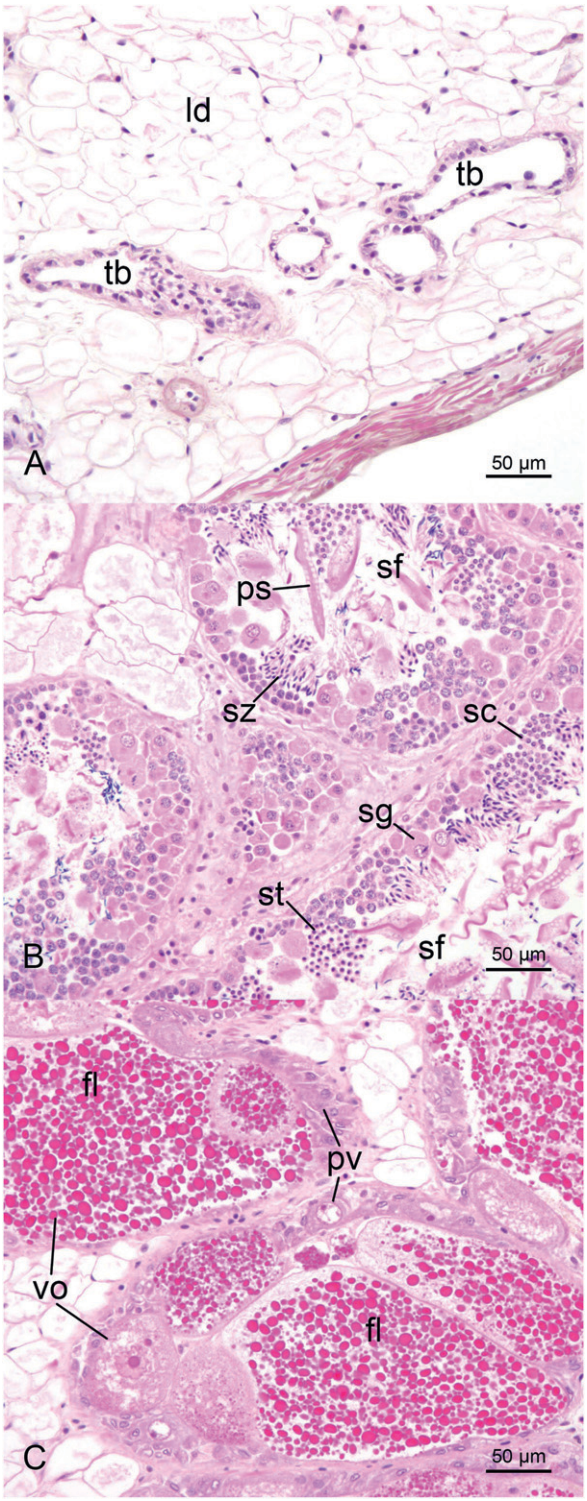

Figure 10. Gonad of *Lobatus gigas*. (A) The inactive gonad consists of connective tissue containing many Leydig cells (ld) and sparse tubules (tb). Sex is based on the presence of a verge and cannot be histologically determined. Davidson's fixative, HE stain. (B) In the male gonad, seminiferous tubules (sf) contain spermatogonia (sg), spermatocytes (sc), spermatids (st), spermatozoa (sz), and paraspermatozoa (ps). Davidson's fixative, HE stain. (C) During oogenesis in the female gonad, oocytes are arranged into follicles (fl). Immature previtellogenic oocytes (pv) are differentiated from mature vitellogenic oocytes (vo) by the absence of yolk granules. Davidson's fixative, HE stain.

the auricle, where it will disperse to the rest of the body. The hemolymph returns from the viscera to the single (right) kidney, for nitrogen excretion, and the urine is excreted through an opening to the mantle cavity, the nephridiopore. The nephridial gland may supplement the formation of urine, particularly in resorption of nutrients, and possibly osmoregulation (Andrews 1988).

The kidney is composed of tall cuboidal to columnar epithelial cells (nephrocytes) that are arranged into ducts and in tubular folds along the dorsal aspect (Fig. 8C). These are supported by a sparse collagenous interstitium that contains many small hemolymphatic vessels and occasional aggregates of pigmented cells (Fig. 8C inset). The brown granular pigment fails to stain for melanin using melanin bleach and Fontana Masson stains or for iron using Perl's stain. Mucus cells may also be present, and those lining the surface and tubular folds may have a microvillus border. The nephrocytes have basal nuclei and variably discretely vacuolated cytoplasm, as observed in other gastropods (Voltzow 1994). The differences in degree of vacuolation can be profound (comparison between Fig. 8C, D), but it is unclear if this represents pathology or physiological variation. The vacuoles may reflect excretory function or pinocytotic vesicles; in other molluscs, these are thought to be involved in glucose resorption (Taylor & Andrews 1987, Andrews 1988). Glycogen storage and glucose resorption seem unlikely because periodic acid-Schiff–positive staining in vacuolated renal epithelial cells was unsuccessful in the authors' experience.

Although the nephridial gland is grossly distinguished from the kidney by its red-brown color (Little 1965), histological distinction is perhaps more vague as the tissues appear similar. Rather than forming lobules as seen in the kidney, nephridial gland is arranged into leaflets that course perpendicular to the longitudinal axis of the gland. The ducts and surface are similarly lined by variably vacuolated cuboidal to columnar cells and mucus cells that are thought to secrete neutral mucopolysaccharides (Andrews 1988) (Fig. 8E). The instititium is similarly sparsely collagenous, highly vascular, and also contains aggregations of pigmented cells. In contrast to the kidney pigment but similar to the rectal mucosa, in the authors' experience, the nephridial gland pigment has stained blue with Perl's stain, indicating the presence of iron. Safe intracellular storage and elimination of iron, likely sourced through dietary algae, may be an important aspect of *Lobatus gigas* physiology that deserves further research.

Heart

The heart is examined in longitudinal section. The myocardium consists of apparently branching striated myocytes, supported by loosely arranged fibrocytes and collagen fibrils, and nerve processes, forming cavernous muscular trabeculae (Fig. 8F). The atrial myocardium may be thinner and more spongy relative to ventricle. The epicardium is composed of simple squamous epithelial cells.

Respiratory System

The gill is examined in a transverse section of mantle that includes the osphradium running in parallel. The gill is composed of a tubular filament that connects to the mantle

(Avila-Poveda et al. 2005) (Fig. 9A, B). The gill of *Lobatus gigas* is monopectinate, bearing triangular lamellae (or leaflets) on one side. Lamellae have cores of vascular loose fibrous connective tissue enclosing small hemolymphatic vessels and are lined by simple cuboidal epithelial cells interspersed with granular gland cells and mucus cells (Fig. 9A). Lamellae flare at their tips (Hyman 1967), and in this region, there is a segment where gill epithelial cells become columnar and have tall cilia (Fig. 9B). The tip of lamellae are supported by skeletal rods, thought to be deposits of basement membrane (Hyman 1967), and may also contain nerve or muscle cells (Voltzow 1994).

The osphradium is a raised ridge of the mantle epithelium centered on a nerve plexus. The central region of the osphradium is considered the sensory component, called the sensory cup (Fig. 9C). Here, there are pseudostratified columnar cells admixed with large mucus cells and cells with homogenous eosinophilic cytoplasm. A cleft separates this area from bordering pseudostratified columnar cells with a microvillus border. Peripheral to this, at the base of the osphradium is a transitional zone containing pigmented cells and a raised ridge of pseudostratified columnar ciliated cells, with clefts at which the nerve processes from the sensory region terminate (Voltzow 1994).

Nervous System

Ganglia and nerves are reliably assessed in serial transverse sections of esophagus and adjacent tissues. The central area of a ganglion consists of neuropil, a tangle of neuronal fibers (Fig. 9D, E). This is peripherally surrounded by a cortical layer composed of a heterogeneous population of large and small neurons. In other prosobranchs, neurosecretory cells have been demonstrated in the cortex using ancillary techniques (Voltzow 1994), but these have not been identified in the queen conch. Neurosecretory cells are neurons that store and secrete hormones. Small aggregations of gray-brown pigmented cells are often adjacent to or within the cortex, confined within the fibrous connective tissue that encapsulates the organ. The brown granular pigment failed to stain for melanin using melanin bleach and Fontana Masson stains.

Nerves consist of parallelly arranged bundles of delicate fibers sparsely populated by nuclei, presumptively representing neuroglia (Fig. 9F). There may be a relatively dense fibrous connective tissue sheath. Some nerves contain quite large axons, producing distinct glassy circular profiles in cross section (Fig. 9F). There are occasional clear spaces around these structures, suggestive of myelin or a similar substance.

Gonad

The gonad is examined in cross section at the edge of the digestive gland. Several reports provide classification systems for the stage of reproductive activity of gonad in *Lobatus gigas* (Aldana-Aranda et al. 2003, Delgado et al. 2004, Avila-Poveda & Baqueiro-Cárdenas 2009). The present study intends only to describe basic cellular elements of the gonad.

In sexually immature individuals of either sex, or in those at a rest (inactive stage of gonad development), sex may be difficult to determine histologically (Aldana-Aranda et al. 2003, Avila-Poveda & Baqueiro-Cárdenas 2009). The gonad consists mostly of connective tissue typically predominated by Leydig cells. There may be few tubuloacini that are lined by undifferentiated low cuboidal germinal epithelial cells (Fig. 10A).

In the male gonad, during spermatogenesis, spermatogonia form seminiferous tubules containing spermatocytes, spermatids, spermatozoa, and paraspermatozoa (Fig. 10B). Similar to the Littorinidae family of marine prosobranchs, *Lobatus gigas* produce flagellate eupyrene spermatozoa, and these may cling to a much larger acrosome-lacking spermatozoa (Hyman 1967), referred to as paraspermatozoa (Voltzow 1994), atypical spermatozoa (Avila-Poveda & Baqueiro-Cárdenas 2009), or nutritious cells (Aldana-Aranda et al. 2003). The function of paraspermatozoa is unknown but may involve provision of nutritive materials to eupyrene spermatozoa, facilitation of their transfer to the female, or preventing their premature dispersal. Developing spermatozoa are known to be supported by Sertoli cells in a number of marine prosobranchs (Buckland-Nicks & Chia 1986), although these are not histologically conspicuous in *L. gigas*. Seminiferous tubules supply ducts (vas deferens) lined by ciliated simple columnar epithelial cells. These may become engorged with spermatozoa during spermatogenesis and may be lost during rest. The number and size of seminiferous tubules, and the proportion of gonad tissue occupied by them, greatly increase over periods of spermatogenesis.

In the female gonad, during oogenesis, germ cells give rise to oogonia that are arranged into follicles (Fig. 10C). Oogonia further differentiate into oocytes. Mature, vitellogenic oocytes are identified by the presence of intracytoplasmic bright eosinophilic vitelline granules that represent accumulation of yolk protein. Follicles supply ducts (oviducts) lined by ciliated simple columnar epithelial cells. These may become distended with vitellogenic oocytes during oogenesis. The number and size of follicles, and the proportion of gonad tissue occupied by them, greatly increase throughout periods of oogenesis.

CONCLUSION

This work highlights the need for greater investigation into the gross and microscopic anatomy and pathology of commercially important gastropods. At present, there is a paucity of literature regarding the microscopic anatomy of Strombidae, limiting structurally distinct versus conserved features of the family. This manual produces a comparative baseline for those investigating the queen conch. It is important that those undertaking postmortem and histological examinations of *Lobatus gigas* communicate their findings so that our limited collective knowledge will be improved.

ACKNOWLEDGMENTS

This work was supported by an intramural grant from Ross University School of Veterinary Medicine, Center for Conservation Medicine and Ecosystem Health. The authors thank the St. Kitts Department of Marine Resources. We are grateful to David Hilchie for helping in histology; to Paul Orchard for

helping in photography; and to Randel Thompson, Maurice Matthew, Kristi Fletcher, Hunter Burns, Tim Courtney, Michelle Farkas, and Aakansha Virwani for their assistance on dissections provided.

LITERATURE CITED

Aldana-Aranda, D., E. Baqueiro-Cárdenas, I. Martínez-Morales, R. I. Ochoa-Báez & T. Brulé. 2003. Gonad behavior during peak reproduction period of *Strombus gigas* from Banco Chinchorro. *Bull. Mar. Sci.* 73:241–248.

Andrews, E. 1988. Excretory systems of molluscs. In: Trueman, E. & M. Clarke, editors. The mollusca, vol. 11. Form and function. New York, NY: Academic Press. pp. 381–448.

Appeldoorn, R. S. 1994. Queen conch management and research: status, needs and priorities. In: Appeldoorn, R. S. & B. Rodriguez, editors. Queen conch biology, fisheries and mariculture. Caracas, Venezuela: Fundacion Cientifica Los Roques. pp. 301–319.

Avila-Poveda, O. H., D. Aldana-Aranda & E. R. Baqueiro-Cárdenas. 2003. Histology of foot epithelium of *Strombus gigas* Linnaeus, 1758. In: Aldana-Aranda, D., editor. El Caracol *Strombus gigas*: conocimiento integral para su manejo sustentable en el Caribe. Merida, Mexico: Programa Iberoamericano de Ciencia y Technologia para el Desarrollo, CYTED. pp. 7–13.

Avila-Poveda, O. H., D. Aldana-Aranda & E. Baqueiro-Cárdenas. 2005. Histological structure of *Strombus gigas* (Gastropoda: Caeaogastropoda: Strombidae). *Proc. Gulf. Caribb. Fish. Inst.* 56:725–739.

Avila-Poveda, O. H., D. Aldana-Aranda & E. R. Baqueiro-Cárdenas. 2006. Histology of selected regions of the alimentary system of *Strombus gigas* Linnaeus, 1758 (Caenogastropoda: Strombidae). *Am. Malacol. Bull.* 21:93–98.

Avila-Poveda, O. H. & E. R. Baqueiro-Cárdenas. 2006. Size at sexual maturity in the queen conch *Strombus gigas* from Colombia. *Bol. Invest. Mar. Cost.* 35:223–233.

Avila-Poveda, O. H. & E. R. Baqueiro-Cárdenas. 2009. Reproductive cycle of *Strombus gigas* Linnaeus, 1758 (Caenogastropoda: Strombidae) from Archipelago of San Andres, Providencia and Santa Catalina, Colombia. *Invertebr. Reprod. Dev.* 53:1–12.

Baqueiro-Cárdenas, E., L. Frenkiel, A. Zetina-Zarate & D. Aldana-Aranda. 2007. Coccidian (apicomplexa) parasite infecting *Strombus gigas* Linne, 1758 digestive gland. *J. Shellfish Res.* 26:319–321.

Boman, E. M., M. D. Graaf, L. A. J. Nagelkerke, A. W. Stoner, C. E. Bissada, O. H. Avila-Poveda, E. R. Baqueiro-Cardenas & A. C. Smaal. 2018. Variability in size at maturity and reproductive season of queen conch *Lobatus gigas* (Gastropoda: Strombidae) in the wider Caribbean region. *Fish. Res.* 201:18–25.

Brownell, W. N. & J. M. Stevely. 1981. The biology, fisheries and management of the queen conch, *Strombus gigas*. *Mar. Fish. Rev.* 43:1–12.

Buckland-Nicks, J. & F. S. Chia. 1986. Fine structure of sertoli cells in three marine snails with a discussion on the functional morphology of sertoli cells in general. *Cell Tissue Res.* 245:305–313.

Cooper, J. E. 2011. Anesthesia, analgesia, and euthanasia of invertebrates. *ILAR J.* 52:196–204.

Cuartas, J. H., J. F. Alzate, C. X. Moreno-Herrera & E. J. Marquez. 2018. Metagenomic analysis of orange colored protrusions from the muscle of queen conch *Lobatus gigas* (Linnaeus, 1758). *PeerJ* 6:e4307.

De Castro, F. & B. Bolker. 2004. Mechanisms of disease-induced extinction. *Ecol. Lett.* 8:117–126.

Delgado, G. A., C. T. Bartels, R. A. Glazer, N. Brown-Peterson & K. J. McCarthy. 2004. Translocation as a strategy to rehabilitate the queen conch (*Strombus gigas*) population in the Florida Keys. *Fish Bull.* 102:278–288.

FAO (Food and Agriculture Organization of the United Nations). 2012. Report of the first meeting of the CFCM/OSPESCA/WECAFC/CRFM working group on queen conch. Accessed May 17, 2018. Available at: www.fao.org/docrep/017/i3193t/i3193t.pdf.

FAO (Food and Agriculture Organization of the United Nations). 2017. Regional queen conch fisheries management and conservation plan. Accessed May 17, 2018. Available at: www.fao.org/3/a-i17818e.pdf.

Glazer, R., N. Denslow, N. Brown-Peterson, P. McClellan-Green, D. Barber, N. Szabo, G. Delgado, K. Kroll, L. Knoebl & D. Spade. 2008. Anthropogenic effects on queen conch reproductive development in South Florida. Marathon, FL: Florida Fish and Wildlife Conservation Commission. 73 pp.

Gros, O., L. Frenkiel & D. Aldana-Aranda. 2009. Structural analysis of the digestive gland of the queen conch *Strombus gigas* Linnaeus, 1758 and its intracellular parasites. *J. Molluscan Stud.* 75:59–68.

Heyliger, H. 1995. Fisheries regulations. In: Heyliger, H., editor. St. Christopher and Nevis Official Gazette. Basseterre, St Kitts: St Christopher and Nevis Government. pp. 1–12.

Howard, D. & C. Smith. 1983. Histological techniques for marine bivalve molluscs. Boston, MA: U. D. o. C. National Oceanic and Atmospheric Administration. 97 pp.

Hyman, L. H. 1967. VIII. Class gastropoda: subclass prosobranchia. In: Hyman, L. H., editor. The invertebrates: mollusca I (volume VI). New York, NY: McGraw-Hill Book Company. pp. 169–384.

Joint, I., M. Mühling & J. Querellou. 2010. Culturing marine bacteria—an essential prerequisite for biodiscovery. *Microb. Biotechnol.* 3:564–575.

Leary, S. 2013. AVMA guidelines for the euthanasia of animals: 2013 edition. Accessed May 17, 2018. Available at: www.avma.org/KB/Policies/Documents/euthanasia.pdf.

Lewbart, G. A. & C. Mosley. 2012. Clinical anesthesia and analgesia in invertebrates. *J. Exot. Pet Med.* 21:59–70.

Little, C. 1965. Notes on the anatomy of the queen conch, *Strombus gigas*. *Bull. Mar. Sci.* 15:338–358.

O'Neal, C. P., B. A. MacDonald, É. Pelletier, R. Saint-Louis & O. S. Phillip 2011. The relationship between imposex and tributyltin (TBT) concentration in *Strombus gigas* from the British Virgin Islands. *Bull. Mar. Sci.* 87:421–435.

Pérez-Carrascal, O. M., M. Posada-Elorza, G. E. Cadavid-Restrepo & C. X. Moreno-Herrera. 2014. Assessment of the bacterial community diversity associated with the queen conch *Strombus gigas* (Linnaeus, 1758) from the Caribbean coast of Colombia using denaturing gradient gel electrophoresis and culturing. *Aquacult. Res.* 45:773–786.

Reed, S. 1993. Gonadal comparison of masculinized females and androgynous males to normal males and females in *Strombus* (Mesogastropoda: Strombidae). *J. Shellfish Res.* 12:71–75.

Reed, S. E. 1995a. Reproductive anatomy and biology of the genus *Strombus* in the Caribbean: I. Males. *J. Shellfish Res.* 14:325–330.

Reed, S. E. 1995b. Reproductive anatomy and biology of the genus *Strombus* in the Caribbean: II. Females. *J. Shellfish Res.* 14:331–336.

Rodriguez, A., H. Hariharan & S. Nimrod. 2011. Occurrence and antimicrobial drug resistance of potential bacterial pathogens from shellfish, including queen conchs (*Strombus gigas*) and whelks (*Cittarium pica*) in Grenada. *Webmed Cent. Microbiol.* 2:WMC001943.

Salvini-Plawen, L. V. 1988. The structure and function of molluscan digestive systems. In: Trueman, E. R. & M. R. Clark, editors. The mollusca, vol. 11, form and function. New York, NY: Academic Press. pp. 301–379.

Spade, D. J., R. J. Griffitt, L. Liu, N. J. Brown-Peterson, K. J. Kroll, A. Reswick, R. A. Glazer, D. S. Barber & N. D. Denslow. 2010. Queen conch (*Strombus gigas*) testis regresses during the reproductive seaszon at nearshore sites in the Florida Keys. *PLoS One* 5:e12737.

Stoner, A. & N. Brown-Peterson. 2012. Histology of queen conch reproductive organs, the Bahamas, 2011 and 2012. Newport, OR: Community Conch. 11 pp.

Stoner, A. W., M. H. Davis & A. S. Kough. 2018. Relationships between fishing pressure and stock structure in queen conch (*Lobatus*

gigas) poulations: synthesis of long-term surveys and evidence for overfishing in the Bahamas. *Rev. Fish. Sci. Aquacult*. 27:1–21.

Stoner, A. W., K. W. Mueller, N. J. Brown-Peterson, M. H. Davis & C. J. Booker. 2012. Maturation and age in queen conch (*Strombus gigas*): urgent need for changes in harvest criteria. *Fish. Res*. 131–133:76–84.

Taylor, P. M. & E. B. Andrews. 1987. Glucose reabsorption by the prosobranch gastropod *Littorina littorea* (L.). *J. Exp. Mar. Biol. Ecol*. 108:99–111.

Theile, S. 2003. Progress on the implementation of the Review of Significant Trade (phases IV and V). Report to the nineteenth meeting of the CITES Animals Committee. Geneva, Switzerland: Convention on International Trade in Endangered Species, CITES. 71 pp.

Tiley, K., M. A. Freeman & M. M. Dennis. 2018a. Pathology and reproductive health of queen conch (*Lobatus gigas*) in St. Kitts. *J. Invertebr. Pathol*. 155:32–37.

Tiley, K., M. M. Dennis, M. R. Lewin-Smith, H. M. Jenkins, Á. Kristmundsson & M. A. Freeman. 2018b. Digestive gland inclusion bodies in queen conch (*Lobatus gigas*) are non-parasitic. *J. Invertebr. Pathol*. 157:4–8.

Volland, J.-M., L. Frenkiel, D. Aldana-Aranda & O. Gros. 2010. Occurrence of sporozoa-like microorganisms in the digestive gland of various species of Strombidae. *J. Molluscan Stud*. 76:196–198.

Volland, J. M., J. P. Lechaire, G. Frebourg, D. A. Aranda, G. Ramdine & O. Gros. 2012. Insight of EDX analysis and EFTEM: are spherocrystals located in Strombidae digestive gland implied in detoxification of trace metals? *Microsc. Res. Tech*. 75:425–432.

Voltzow, J. 1994. Gastropoda: Prosobranchia. In: Harrison, F. W. & A. J. Kohn, editors. Microscopic anatomy of invertebrates: vol. 5: mollusca one: monoplacophora, aplacophora, polyplacophora and gastropoda. New York, NY: Wiley-Liss. pp. 111–252.

Wilbur, K. 1972. Shell formation in mollusks. In: Florkin, M. & B. Scheer, editors. Chemical zoology, vol. VII mollusca. New York, NY: Academic Press. pp. 235–287.